Journal of Atmospheric Chemistry (2023) 80:173–189
https://doi.org/10.1007/s10874-023-09446-7

Fate of 1,3-dioxolane in the troposphere: kinetics, mechanism with theoretical support, and atmospheric implications

Anmol Virmani[1] · Mohini P. Walavalkar[1] · Asmita Sharma[1] · Ankur Saha[1,2] · Sumana Sengupta[1,2] · Awadhesh Kumar[1,2]

Received: 30 November 2022 / Accepted: 21 March 2023 / Published online: 12 April 2023

Abstract

The atmospheric fate of 1,3-dioxolane is assessed by measuring the OH and Cl initiated gas-phase oxidation kinetics, and exploring their mechanistic pathways. Absolute OH reaction rate coefficient of 1,3-dioxolane using laser photolysis-laser induced fluorescence technique is found to be $(1.27 \pm 0.03) \times 10^{-11}$ cm^3 molecule^{-1} s^{-1} at 298 ± 2 K and it is in good agreement with the measured relative value of $(1.13 \pm 0.12) \times 10^{-11}$ cm^3 molecule^{-1} s^{-1}, using gas-chromatography. Relative value of Cl reaction rate coefficient with 1,3-dioxolane is found to be $(1.64 \pm 0.60) \times 10^{-10}$ cm^3 molecule^{-1} s^{-1}. The tropospheric lifetime of 1,3-dioxolane is calculated to be about 22 h under ambient conditions. Interestingly, it reduces to about 8 h near marine boundary layer, where Cl reaction takes over the OH reaction. Such a short lifetime with respect to reaction with OH and Cl suggests the atmospheric impact of 1,3-dioxolane to be local. Formic acid, ethylene carbonate, and 1,2-ethanediol monoformate are observed as stable products in OH as well as Cl oxidation. 1,3-dioxolane may contribute as one of the sources of formic acid in the atmosphere. Theoretical calculations for the OH-initiated hydrogen abstraction of 1,3-dioxolane revealed that the reaction follows an indirect path through the formation of pre- and post-reaction complexes at entrance and exit channels, respectively with the lowest barrier height of 3.5 kcal/mol. Photochemical ozone creation potential of 1,3-dioxolane is calculated.

Keywords 1,3-dioxolane · Kinetics · LP-LIF · Rate coefficient · Theoretical calculations

✉ Ankur Saha
ankurs@barc.gov.in

✉ Awadhesh Kumar
awadesh@barc.gov.in

[1] Radiation & Photochemistry Division, Bhabha Atomic Research Centre, Trombay, Mumbai 400085, India

[2] Homi Bhabha National Institute, Anushaktinagar, Mumbai 400094, India

1 Introduction

Volatile organic compounds (VOCs) are emitted into the atmosphere via a variety of natural, anthropogenic, and biogenic sources (Graedel et al. 1986) and can be a potential source of environmental concerns such as global warming, ozone depletion, and photochemical smog. Tropospheric lifetime of a VOC is an important factor to study its transport and distribution in the atmosphere. It is also related to global warming potential (GWP) for any VOC (Hodnebrog et al. 2013). It is decided by the collective contribution of all the possible degradation processes for any VOC. Common degradation processes are wet deposition, photodissociation, and oxidation by tropospheric oxidants. Tropospheric lifetime of majority of VOCs is mainly determined by the kinetics of their gas phase oxidation with the OH radical (Calvert et al. 2002). The OH radical can either add on to the double bonds of a VOC or abstract hydrogen atoms leading to short lived radicals, which decompose to smaller fragments or react with other available molecules. Water soluble VOCs can be washed out by rain. Near marine boundary layer (MBL), oxidation by Cl radicals can be the major degradation channel for a VOC (Spicer et al. 1998). Therefore, it is required to have a precise and accurate value of rate coefficient for reaction of a VOC with these oxidants in order to ascertain its environmental impact.

Ethers are an important class of VOCs, which are used as industrial solvents and fuel additives in the automobile industry in order to decrease the pollutants such as CO, particulates etc., in the exhaust of automobiles (Dolislager 1997). Discovery of methyl tert-butyl ether (MTBE) in groundwater and reservoirs used for drinking (Squillace et al. 1996) manifests the widespread usage of ethers and thereby studies are required to assess their possible environmental impact. Here in this work, we have determined the rate coefficients of a cyclic

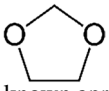

ether namely 1,3-dioxolane with the OH and Cl radical. 1,3-dioxolane is a well-known aprotic solvent to the chemists. It is used for dissolving various polar polymers such as polyester, polyurethanes, and epoxides (Gupta et al. 2016). It is also used as an extractant for waxes, fats and oils, stabilizer for halogenated hydrocarbons and comonomer in polyacetals preparation (Cheremisinoff 2003). Its excellent solvency makes it an important constituent in paint removal formulations and as a carrier fluid in film coatings (Cheremisinoff 2003). It is used as a finishing agent and swelling agent in textiles (Andrews 1987). Poly(1,3-dioxolane) based deep-eutectic polymer electrolytes are used for high performance ambient polymer lithium battery (Wang et al. 2022). It acts as an intermediate for the preparation of anti-HIV pharmaceuticals like diaminopurine dioxolanes and dioxolane thymines (Andrei et al. 2017). There is a report on the soot reducing properties of 1,3-dioxolane as a diesel additive (Song et al. 2004). 1,3-dioxolane is also used as a promoter for CO_2 clathrate hydrate formation (Torré et al. 2015). This compound is known to enhance the dielectric and optical anisotropy in tolane-liquid crystals (Chen et al. 2015). There are reports on the potential antibacterial and antifungal activities of substituted 1,3-dioxolanes (Küçük et al. 2011; Ovsyannikova et al. 2013). Therefore, it is crucial to determine its atmospheric indices for the evaluation of its possible environmental impact. There are reports in the literature concerning the measurement of the rate coefficient of 1,3-dioxolane with the OH radical (Moriarty et al. 1999; Sauer et al. 1999; Dinis et al. 2001; Calve et al. 2002). Room temperature absolute rate coefficient for the aforementioned reaction at 295 K has been reported to be $(11.8 \pm 0.5) \times 10^{-12}$ cm^3 molecule^{-1} s^{-1} and $(11.1 \pm 0.3) \times 10^{-12}$ cm^3 molecule^{-1} s^{-1} by Moriarty et al. and Le Calve et al., respectively. While Sauer et al. and Dinis et al. reported the absolute rate coefficient to be $(8.8 \pm 0.9) \times 10^{-12}$ cm^3 molecule^{-1} s^{-1} and $(7.9 \pm 0.4) \times 10^{-12}$ cm^3 molecule^{-1} s^{-1},

respectively. It is worth noting that absolute value of the rate coefficient reported by Sauer et al. and Dinis et al. differs from that reported by Moriarty et al. and Le Calve et al. The rate coefficient reported by Moriarty et al. is 1.5 times greater than that reported by Dinis et al. To get a more consistent rate coefficient value, we have carried out multiple measurements of the OH radical reaction rate coefficient using both absolute and relative rate methods. There is a good agreement between our measured values of absolute and relative rate coefficient, which matches closely with that reported by Moriarty et al. There is only one report on the rate coefficient for the reaction of 1,3-dioxolane with Cl atom to be $(1.6 \pm 0.3) \times 10^{-10}$ cm^3 $molecule^{-1}$ s^{-1} by Sauer et al. We have used relative rate method to measure the Cl atom reaction rate coefficient and our reported value matches with that reported by Sauer et al. The kinetics data are used to estimate net tropospheric lifetime of 1,3-dioxolane. There is a report on the mechanistic studies of the reaction of 1,3-dioxolane with the OH and Cl, in presence of NO, using FT-IR spectroscopy by Sauer et al. We have revisited the possible degradation products of the reaction of 1,3-dioxolane with OH and Cl in the presence of air at atmospheric pressure, using GC–MS technique. We have also calculated the photochemical ozone creation potential (POCP) of 1,3-dioxolane. Apart from this, for a better understanding of mechanistic pathways, kinetics and thermochemistry, we have carried out theoretical studies to map the potential energy surface of the H-abstraction reaction of 1,3-dioxolane by OH involving possible pre- and post-reactive complexes, and transition states. This is the first computational study providing the detailed information of kinetic pathways of the reaction of 1,3-dioxolane with the OH radical.

2 Experimental

2.1 Kinetic studies using absolute rate method

Bimolecular rate coefficient for the reaction of 1,3-dioxolane with the OH radical was measured by performing kinetic measurements under pseudo first-order conditions by using Laser Photolysis-Laser Induced Fluorescence (LP-LIF) technique, under flow conditions. The experimental details of the LP-LIF set up are given in our earlier publications (SenGupta et al. 2010). A brief account of the experimental details is also mentioned here. The experimental procedure involves the measurement of the rate of OH decay in the absence and presence of the VOC. A known flow of 1,3-dioxolane in N_2 buffer gas was introduced in the premix chamber. A constant flow of N_2 gas was bubbled through approximately 50% H_2O_2 solution using a calibrated mass flow controller, and then passed to the reaction cell through the premix chamber. A known pressure of 1,3-dioxolane sample in N_2 buffer gas was then introduced in the premix chamber, so that the sample, H_2O_2, and N_2 get mixed before entering the reaction cell. The reaction cell is made up of a double-walled jacketed glass fitted with MgF_2 windows kept at the Brewster angle to minimize scattering. In the blank experiment, H_2O_2 seeded in N_2, and buffer N_2 were flown through the reaction cell, without the sample, and the decay kinetics of OH were measured. Here the decay of OH concentration is due to diffusion out of the detection zone and its reaction with H_2O_2. The OH radicals were generated by the photolysis of H_2O_2 at 248 nm (KrF excimer laser, Lambda Physik, Compex 102) operated at 20 Hz with fluence of 0.2–0.8 mJ/cm^2. These radicals were excited by a probe laser tuned to around 308 nm with the energy low enough (20 μJ/Pulse) to avoid saturation of the transition. The probe laser was operated on the frequency doubled output of a DCM special dye (Lambdachrome, LC 6501, 590–640 nm) and pumped by the second harmonic of an Nd:YAG laser (Quantel,

YG980). Both the photolysis and the probe laser beams were aligned to intersect in the center of the cell at the right angle, and pass through the exit windows. The $P_1(2)$ rotational line of the $A \rightarrow X$ (0–0) vibrational band of the OH radical was excited near 308 nm and the resulting fluorescence was collected using a photomultiplier tube in combination with a lens and a band pass filter centred at 310 nm. Decay kinetics of OH was followed by plotting the fluorescence intensity as a function of time delay between the photolysis and the probe laser using a delay generator with delay range of 10 μs to 10 ms, in steps of a few microseconds. The fluorescence signal was gate integrated by a boxcar (SRS 20), averaged over 50 laser shots, and fed into an interface (SRS 245), for A/D conversion. A PC was used to control the scan of the dye laser via an RS232 interface, and to collect data through a GPIB interface, using a control and data acquisition program. The pressure inside the cell was measured with a capacitance manometer and was kept near 20 Torr with a total flow rate of 150 SCCM. Subsequently, a known pressure of 1,3-dioxolane in N_2 buffer gas was flown in the reactor, and the OH decay kinetics was recorded. Sufficient flow velocity of the experimental mixture was maintained (~ 12 cm/sec) to allow sampling of a fresh gas mixture by each photolysis laser pulse.

2.2 Kinetic studies using relative rate method

In the relative rate method, the rate coefficient for the reaction of the sample with the oxidant is measured with respect to a reference, whose rate coefficient with that oxidant is well reported. Gas chromatography is used for detection and separation of the species involved in the reaction employing capillary (fused silica) carbowax columns under suitable conditions of temperature and flow. We have used a quartz reaction cell for carrying out relative rate experiment which consists of 1,3-dioxolane (100 – 150 ppm), reference molecule (50 – 150 ppm), and $(COCl)_2$/ (O_3-H_2O mixture) (400–500 ppm) along with buffer gas (N_2 / air). Photolysis of $(COCl)_2$ and (O_3-H_2O) at 254 nm was done in situ for generating Cl and OH radicals respectively. Delay between the photolysis and analysis time was kept to the minimal to prevent any ozone side reaction with the sample and the reference. The total pressure was maintained at 800 ± 3 Torr. Cyclohexane was used as a reference compound for OH while Ethene and 1-butene were used as reference compounds for Cl, after satisfying the conditions required for measuring the rate coefficient by relative rate method. The kinetic data for the reaction of the 1,3-dioxolane (DXL) with the oxidant is measured using the standard expression:

$$\ln\left(\frac{[DXL]_{t=0}}{[DXL]_t}\right) = \frac{k_{DXL}}{k_R}\ln\left(\frac{[R]_{t=0}}{[R]_t}\right) \quad (1)$$

Here, $[R]_t$ and $[DXL]_t$ are concentrations of reference compound and 1,3-dioxolane, respectively, at time t, and $[R]_{t=0}$ and $[DXL]_{t=0}$ are the corresponding initial concentrations.

3 Results and discussion

3.1 Rate coefficient measurement using absolute method by LP-LIF technique

The various processes responsible for the decay of OH concentration is accounted by the below mentioned equations:

$$OH + C_3H_6O_2 \overset{k_{DXL}}{\rightarrow} C_3H_5O_2 + H_2O \quad (2)$$

$$OH + H_2O_2 \overset{k_1}{\rightarrow} HO_2 + H_2O \tag{3}$$

$$OH \overset{k_d}{\rightarrow} diffusion\ out\ of\ the\ detection\ volume \tag{4}$$

where k_{DXL}, k_1, and k_d are the rate coefficients for the reaction of 1,3-dioxolane with OH, H_2O_2, and diffusion process, respectively. The rate of decrease in the OH concentration is given as,

$$-\frac{d[OH]}{dt} = \left(k_{DXL}\left[C_3H_6O_2\right] + k_1\left[H_2O_2\right] + k_d\right)[OH] \tag{5}$$

In all the experiments, the conditions, $k_{DXL}[C_3H_6O_2][OH] >> k_1[H_2O_2][OH]$, $[H_2O_2] \approx$ constant and the total pressure = constant, are maintained. Thus, the above equation simplifies to

$$-\frac{d[OH]}{dt} = (k_{DXL}[DXL] + k_d^{'})[OH] \tag{6}$$

where $k_d^{'}$ represents $k_1\left[H_2O_2\right] + k_d$. Since [OH] << [1,3-dioxolane] we have $k_{DXL}[DXL] + k_d^{'} = k'$ (pseudo-first order rate coefficient), and solving the differential equation leads to

$$[OH]_t = [OH]_0 \exp\left(-k^{'} t\right) \tag{7}$$

Values of k' at a particular temperature is obtained by plotting the log plot of decay of [OH] vs time as shown in Fig. 1. Here, the LIF signal is propotional to the concentration of OH radical for a given pump-probe delay. Three to four decays were recorded corresponding to a certain [1,3-dioxolane] and average of k' obtained vs [1,3-dioxolane] is plotted in the Fig. 2 for a set of at least three measurements. The slope of this plot gives k_{DXL}. At room temperature, the value of $k_{DXL}(298 \pm 2\ \mathrm{K})$ was found to be $(1.27 \pm 0.03) \times 10^{-11}$ cm^3 $molecule^{-1}$ s^{-1}. The error corresponds to 2σ of the linear regression and is devoid of any systematic errors, such as the errors in measuring flow rates, partial pressures which can be up to 5%.

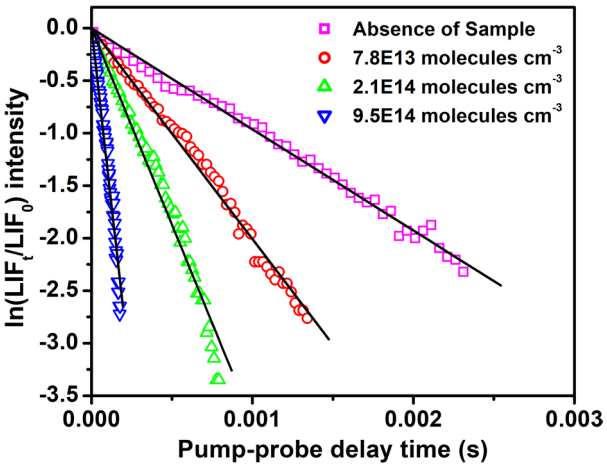

Fig. 1 Typical decay profiles of the OH radical at 298 ± 2 K, in absence and with increasing concentration of 1,3-dioxolane as shown in various curves. LIF signal is proportional to the concentration of OH radical. These curves fit into the first-order kinetics equation, shown as solid lines

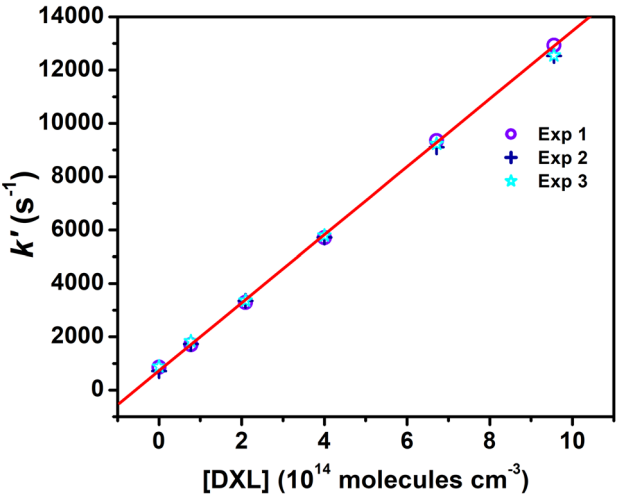

Fig. 2 Plot of the pseudo first-order rate coefficient, *k'* vs [DXL] for temperature 298 ± 2 K and 20 Torr pressure for different set of experiments. Each point represents the average of three to four measurements of the first order decay at a particular number density of the sample

3.2 Rate coefficient measurement using relative method by GC

The relative value of rate coefficient of the reaction of an oxidant with any sample compound depends explicitly on the absolute value of reference rate coefficient. We have chosen the recommended value of reference rate coefficient from the available database on kinetics of such bimolecular reactions (McGillen et al. 2020). The rate coefficients for the reactions of OH at 298 K with reference compound cyclohexane is taken to be $(6.69 \pm 0.67) \times 10^{-12}$ cm^3 molecule^{-1} s^{-1} (McGillen et al. 2020). The rate coefficient for the reactions of Cl atom at 298 K with the reference compounds, ethene and 1-butene, is taken to be $(1.06 \pm 0.03) \times 10^{-10}$ cm^3 molecule^{-1} s^{-1} (Atkinson and Aschmann 1985; McGillen et al. 2020) and $(3.0 \pm 0.4) \times 10^{-10}$ cm^3 molecule^{-1} s^{-1} (Daranlot et al. 2010; McGillen et al. 2020), respectively. The typical relative rate plot for the decay of 1,3-dioxolane with cyclohexane as a reference molecule is shown in Fig. 3, with N_2 as a buffer gas. The typical relative rate plot for the decay of 1,3-dioxolane with ethene and 1-butene as reference molecules is shown in Fig. 4. The slopes of the linear least square fits correspond to the ratios of the rate coefficients, $k_{DXL}/k_{reference}$, and the average values of k_{DXL} are listed in Table 1. The quoted error in the rate coefficient includes the reported error in the reference rate coefficients as well.

3.3 Tropospheric lifetime

The atmospheric lifetimes of majority of the VOCs mainly depend on their reactions with the tropospheric oxidants. The lifetimes, τ_i of a VOC due to its reaction with the individual tropospheric oxidant is given by,

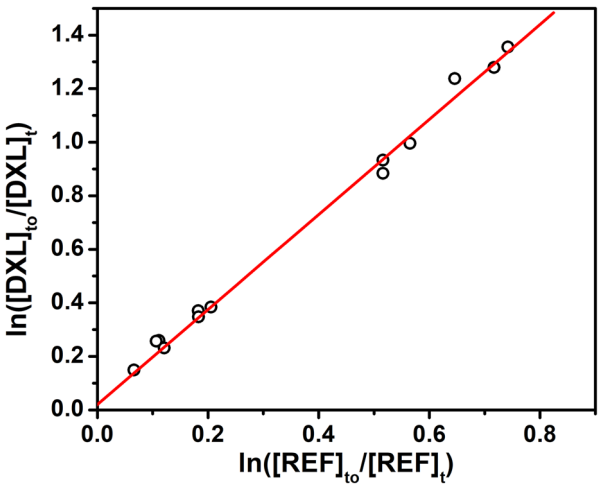

Fig. 3 Fractional decrease in the concentration of 1,3-dioxolane with respect to cyclohexane in presence of 800 Torr of N_2. Slope of the straight line is 1.78 ± 0.02

$$\tau_{Oxidant}^{VOC} = \frac{1}{k_{Oxidant}^{VOC} \times [Oxidant]} \tag{8}$$

So, the lifetime of 1,3-dioxolane (DXL) due to its reaction with OH and Cl can be written as

$$\tau_{OH}^{DXL} = \frac{1}{k_{OH}^{DXL} \times [OH]} \text{ and } \tau_{Cl}^{DXL} = \frac{1}{k_{Cl}^{DXL} \times [Cl]} \tag{9}$$

Here, τ_{OH}^{DXL} and k_{OH}^{DXL} are the tropospheric lifetime and the rate coefficient of 1,3-dioxolane for removal by OH radicals, respectively, and τ_{Cl}^{DXL} and k_{Cl}^{DXL} are the tropospheric lifetime and the rate coefficient of 1,3-dioxolane for removal by Cl atoms, respectively. In terms of the individual tropospheric lifetimes, τ_i, the overall tropospheric lifetime, τ, is calculated using the formula

$$\tau = [\sum\nolimits_i (\tau_i)^{-1}]^{-1} \tag{10}$$

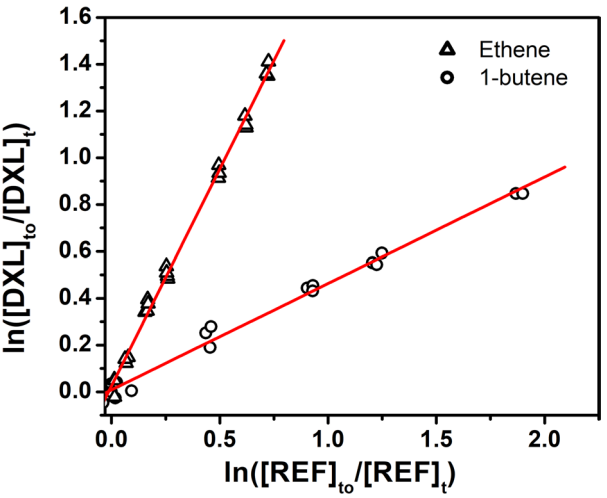

Fig. 4 Fractional decrease in the concentration of 1,3-dioxolane with respect to ethene (open triangle) and 1-butene (open circle) in presence of 800 Torr of N_2

Table 1 Relative rate ratios and rate coefficients calculated at room temperature for DXL + OH/CL

Oxidant	Reference	k_{DXL}/k_R	Rate coefficient k_{DXL} (cm^3 $molecule^{-1}$ s^{-1})
OH	Cyclohexane	1.78 ± 0.02	$(1.19 \pm 0.12) \times 10^{-11}$
		1.67 ± 0.03	$(1.12 \pm 0.11) \times 10^{-11}$
		1.62 ± 0.04	$(1.08 \pm 0.11) \times 10^{-11}$
		1.69 ± 0.05 (average)	**$(1.13 \pm 0.12) \times 10^{-11}$**
Cl	Ethene	1.86 ± 0.03	$(1.97 \pm 0.06) \times 10^{-10}$
		1.60 ± 0.04	$(1.70 \pm 0.06) \times 10^{-10}$
		1.77 ± 0.13	$(1.88 \pm 0.15) \times 10^{-10}$
		1.74 ± 0.14 (average)	**$(1.85 \pm 0.16) \times 10^{-10}$**
Cl	1-Butene	0.45 ± 0.01	$(1.35 \pm 0.54) \times 10^{-10}$
		0.51 ± 0.01	$(1.53 \pm 0.61) \times 10^{-10}$
		0.48 ± 0.01	$(1.44 \pm 0.58) \times 10^{-10}$
		0.48 ± 0.02 (average)	**$(1.44 \pm 0.58) \times 10^{-10}$**
		Average value of Cl rate coefficient: **$(1.64 \pm 0.60) \times 10^{-10}$**	

Average values are depicted in boldface

The average atmospheric OH concentration, [OH], is considered as 1.0×10^6 molecules cm^{-3} (Prinn et al. 2001). OH and Cl reactions are considered for evaluation of tropospheric lifetime, which is found to be around 22 h for 1,3-dioxolane. The tropospheric lifetime of 1,3-dioxolane with respect to Cl atom is calculated under both the ambient and the MBL conditions to be 1500 h and 13 h, taking [Cl] to be 1×10^3 and 1.3×10^5 molecules cm^{-3}, (Sharma et al. 2011), respectively. Hence, Cl atom reaction becomes the predominant sink under MBL conditions and the overall lifetime of 1,3-dioxolane is reduced to 8 h. For any compound to be transported across different regions, global atmospheric emissions, gas-particle partitioning, and lifetime with respect to different tropospheric removal channels play a major role (Lohmann et al. 2007). For example, gaseous compounds undergo much faster OH radical reaction than those associated with particle phase. As a consequence, more volatile organics are removed faster. There are reports on the real time analysis of concentration of cyclic ethers like ethylene oxide (Hasegawa 2001) and aromatic ethers like polybrominated diphenyl ethers (Su et al. 2007; Schure et al. 2004) over different regions. The presence of such ethers in the atmosphere is particularly due to significant global emissions and atmospheric residence time of several days. 1,3-dioxolane has a very short lifetime with respect to reaction with OH and Cl and as a result its concentration does not build up in the atmosphere. Hence, its atmospheric impact is locally concentrated on its emission zones. Also, such a short lifetime suggests that 1,3-dioxolane will not contribute to the radiative burden of the atmosphere. We have also calculated the Global warming potential (GWP) (Section S2 of supplementary material) and found it be 0.18 for 100-year time horizon.

3.4 Stable product analysis

The products of the reaction of 1,3-dioxolane with Cl and OH formed in the presence of air at atmospheric pressure, were characterized by a Gas Chromatograph coupled with a Mass Spectrometer (Shimadzu), using CPWAX 52CB (30 mm × 0.25 mm × 0.25 μm) capillary columns, with appropriate temperature programming, for separation of the products. The

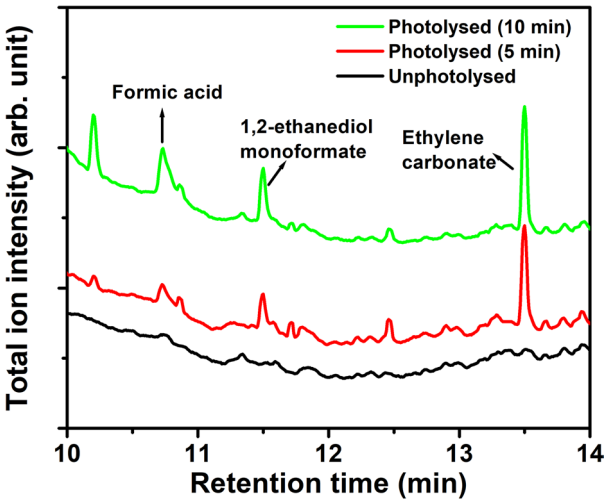

Fig. 5 Total ion chromatogram of products of reactions of 1,3-dioxolane with OH radical precursor before and after photolysis (that is, reaction with OH radical). Spectra have been vertically translated for clarity

observed spectral features of the detected products were then compared with the reported mass spectra for identification purpose. In the present study using GC–MS, the products observed in OH oxidation are formic acid, 1,2-ethanediol monoformate, and ethylene carbonate with retention time at 10.7 min, 11.5 min, and 13.4 min respectively. In addition to these products, one more unidentified product with retention time at 10.2 min was obtained. A typical chromatogram of products of OH reaction is shown in Fig. 5. Among the three identified products, formic acid, 1,2-ethanediol monoformate are the products formed by ring opening of primary radical formed by abstraction and ethylene carbonate is formed by oxidation of the radical formed by abstraction from second position (Fig. 6).

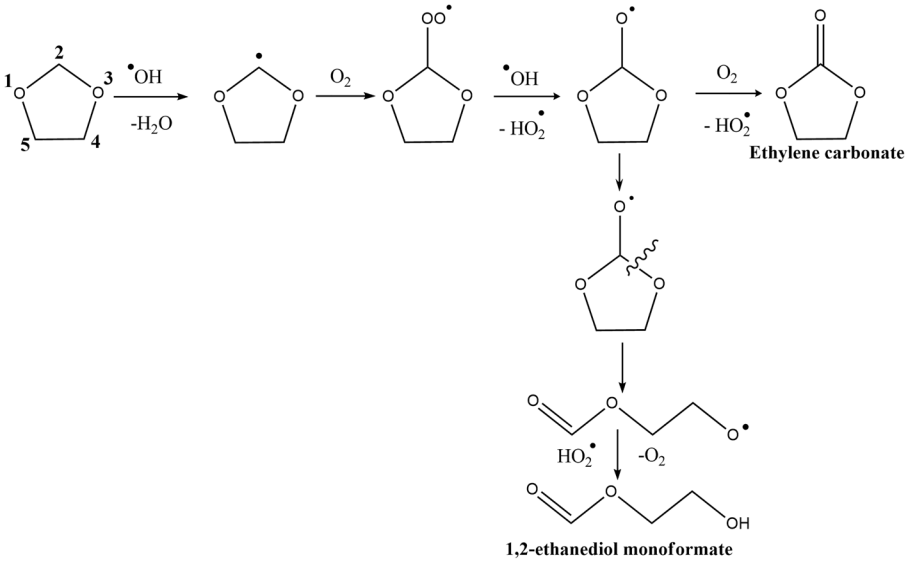

Fig. 6 Probable mechanism for the formation of ethylene carbonate and 1,2-ethanediol monoformate from the reaction of 1,3-dioxolane with OH radical

Same identified products are obtained in case of Cl radical reaction also along with two unidentified products at the same position with the same mass spectra indicating the mechanism of the reaction of 1,3-dioxolane with both the oxidants to be similar. The exact detailed mechanism of such abstraction reaction can be elucidated by studying chemical dynamics using Velocity map imaging (VMI) measurements and quasi-classical trajectory (QCT) calculations on the potential energy surface (PES) (Pandit et al. 2017).

3.5 Theoretical calculations

Ab initio MO calculations are performed using the Gaussian 03 program suite (Frisch et al. 2004). Geometries of the involved reactants, intermediate complexes, transitions states, and products were optimised at the B3LYP/6-311G(d,p) level of theory. Single point energy is calculated at the QCISD level using the same basis sets. The authenticity of the transitions states was ascertained by presence of only one imaginary frequency and one negative eigenvalue of the force constant matrix. Intrinsic reaction coordinate (IRC) calculations were also done at the B3LYP/6-311G(d,p) level of theory to check if a transition state corresponds with its desirable minima (Fig. S1 of supplementary material). No spin contamination was found in any of the species involved in the reaction. The 1,3-dioxolane molecule has 6 abstractable hydrogen atoms, which can serve as the sites for the OH reaction. Because of the puckered structure (C_1 point group) of 1,3-dioxolane, it is not possible to assign the symmetry of hydrogen atoms based on their chemical environment. So, we calculated the energies of the transition states for each H atom abstraction. We found that the transition states corresponding to hydrogen atoms labelled as H_1, H_2 have similar energies. Similarly, transition states corresponding to H_3, H_5 and H_4, H_6 have similar energies. Hence, for H atom abstraction process, we will be presenting the TS structures for H_1, H_4, and H_5 abstraction only. Structures of TS corresponding to H_2, H_3, H_6 abstraction are shown in Fig. S3 of supplementary material. The potential energy curves for the abstraction of H atoms by OH are also shown in Fig. 7. The reaction was found to proceed through

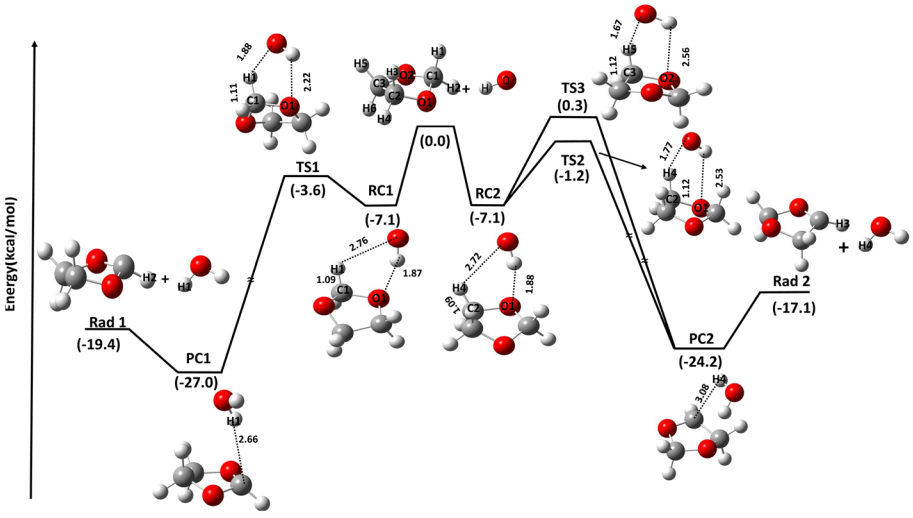

Fig. 7 Energy profile for the 1,3-dioxolane + OH reaction calculated at the QCISD/6-311G(d,p) level of theory. Bond distances are in Å

a pre-reactive van der Waals complex. Generally, such complexes are more often found in the addition reactions of alkenes with the OH radical (Senosiain et al. 2006; Zhang et al. 2019). However, there are reports on the presence of such complexes in H-abstraction reactions of oxygenated (Kawade et al. 2018a, b) and non-oxygenated VOCs (Szori et al. 2007). We could optimise two reaction complexes (RC1, RC2) for the above reaction, each stabilised by 7.1 kcal/mol with respect to the reactants. H-bonding interactions between H atom of OH with the O atom of 1,3-dioxolane are responsible for the stability of the complexes. Kawade et al. obtained a value of 5.3 kcal/mol at G3 level of theory for the stability of reactant complex of dimethyl ether with the OH radical (Kawade et al. 2018a). RC1 involves H-bond interaction between the H atom of OH and O1 atom of the dioxolane ring with a distance of 1.87 Å. This complex also involves interaction between the O atom of OH with the H atom on C1 of 1,3-dioxolane. Subsequently, RC1 is converted to the product-complex PC1 (-27.0 kcal/mol with respect to the reactants) via the TS (TS1) with activation barrier of 3.5 kcal/mol. PC1 eliminates H_2O to form a radical (Rad 1) with an overall exothermicity of 19.4 kcal/mol. Similar to RC1, RC2 involves H-bond between the H atom of OH and O1 atom of the dioxolane ring with a distance of 1.88 Å. The reactant-complex RC2 also gets further stabilised to the product-complex PC2 (24.2 kcal/mol) involving TS structure TS2 with activation barrier of 5.9 kcal/mol.

Similar to TS2, TS3 proceeds through an intermediate complex (not shown in Fig. 7) that is structurally and energetically similar to RC2. Finally, PC2 dissociates to the final products, Rad $2 + H_2O$, with an overall exothermicity of 17.1 kcal/mol. Between two radicals formed after H atom abstraction, Rad 1 is more stable than Rad 2 and the higher stability of the former can possibly be explained based on inductive and hyperconjugation effects. Rad 1 is stabilised by inductive effect from the two neighbouring oxygen atoms. But Rad 2 lacks these cooperative inductive effects, and has stability due to relatively weak hyperconjugation effect and inductive effect from one oxygen atom. The relative stability of these radicals is observed in their respective TS structures as well with TS1 (-3.6 kcal/mol) being more stable than TS2 (-1.2 kcal/mol) and TS3 (0.3 kcal/mol). Our calculations predict an effective activation barrier of 3.5, 5.9, and 7.4 kcal/mol for the H atom abstraction reactions through the transition states TS1, TS2, and TS3, respectively. The expected most probable abstraction reaction channel has the lowest value of activation barrier via TS1 with the shortest O(1,3-dioxolane)-H(OH) bond distance of 2.22 Å compared to 2.53 Å and 2.56 Å in TS2 and TS3. The fact that the elongation of forming bond is larger than that of the breaking bond indicates that the barrier of the reaction is near the corresponding reactants. This implies that the reaction will proceed via an early barrier with the transition state structure resembling the reactant structure. This is in consonance with the Hammond's postulate expected for a highly exothermic hydrogen abstraction reaction (Hammond 1955). Such hydrogen abstraction reactions from ethers might show negative temperature dependence due to the formation of a stable pre-reactive complex (Ill´es et al. 2021; Moriarty et al. 2003; Porter et al. 1997). We could also optimize a pre-reactive complex for the reaction of 1,3-dioxolane with the OH radical. However, rate coefficient of this reaction is reported to be independent of temperature in the range of 250–550 K, within the experimental uncertainties (Dinis et al. 2001). Such kind of abstraction reactions are mostly pressure independent (Kawade et al. 2017) and can be ignored for model calculations in tropospheric chemistry (Klein et al. 1984). Pressure dependence is often found in the reaction involving some adduct that can undergo collisional activation/deactivation (Persis et al. 2004).

At this point, it will be interesting to compare the rate coefficients of the reaction of the OH radical with dimethoxy methane and dimethoxy ethane (linear analogues

of 1,3-dioxolane). The rate coefficients of the OH radical with dimethoxy methane ($CH_3OCH_2OCH_3$) (Wallington et al. 1997) and dimethoxy ethane ($CH_3OCH_2CH_2OCH_3$) (Porter et al. 1997) are reported to be $(0.53 \pm 0.1) \times 10^{-11}$ cm^3 $molecule^{-1}$ s^{-1} and $(2.8 \pm 0.1) \times 10^{-11}$ cm^3 $molecule^{-1}$ s^{-1}, respectively. The rate coefficient of the OH radical with 1,3-dioxolane is about two times faster than that with dimethoxy methane but about two times slower than that with dimethoxy ethane. The H-atom abstraction reaction of dimethoxy methane can proceed through a five-membered transition involving O-CH_2. However, in such a case, there will be steric hindrance from the neighbouring methyl groups that will destabilise the transition state. As a result, the reaction is expected to be slower. In addition, the presence of some strain energy in the cyclic 1,3-dioxolane can also enhance its rate coefficient. However, the rate coefficients of the OH radical with dimethoxy ethane is around two times faster than that with 1,3-dioxolane. The formation of more stable six-membered transition state with H-bonding between H atom of OH with the O atom of dimethoxy ethane and the absence of steric crowding could be responsible for a greater rate coefficient.

3.6 Photochemical ozone creation potential

Photochemical ozone creation potential (POCP) value for a given VOC assesses its ability to form ozone relative to ethene for same atmospheric mass emission (Derwent and Jenkin 1991). Recently, Jenkin et al. proposed the following expression for POCP calculation (Jenkin et al. 2017):

$$POCP = (A \times \gamma S \times R \times S \times F) + P + R_{O3} - Q \tag{11}$$

F is a parameter that accounts for the impact of unreactive carbonyl product formation and is generally taken to be 1. The parameter P is only applied to emitted carbonyl compounds and takes a value of zero in our case of 1,3-dioxolane. R_{O3} accounts for the formation of free radicals from the VOCs reaction with ozone and hence assumes zero value in our case. Q applies only to a specific set of aromatic VOCs and is generally taken as zero. γS is VOC structure dependent parameter given by

$$\gamma S = \left(\frac{n_B}{6}\right) \times \left(\frac{28.05}{M}\right) \tag{12}$$

where n_B is the number of C–C and C-H bonds in one VOC molecule and M is its molecular mass.

R is related to rate coefficient of the VOC with the OH radical, and is given by

$$R = 1 - (B.\gamma_R + 1)^{-1} \tag{13}$$

and

$$\gamma_R = \left(\frac{k_{OH}}{k_{OH}*}\right) \times \left(\frac{6}{n_B}\right) \tag{14}$$

where k_{OH} is the rate coefficient for VOC reaction with OH at 298 K and atmospheric pressure, $k_{OH}*$ is the same quantity for the reference VOC, ethene.

S is determined by the size of the compounds and is given as:

$$S = (1 - \alpha) \times \exp\left(-C \times {n_C}^{\beta}\right) + \alpha \quad (15)$$

n_C is the number of carbon atoms of the VOC. A, B, α, β are varied and optimized to VOC size dependence of POCP values over northwestern European conditions and US urban conditions over differing timescales.

1,3-dioxolane has chemical formula $C_3H_6O_2$ with mol. wt. 74.05 g/mol and has 1 C–C bond and 6 C-H bonds and 3 carbon number. Therefore, $n_B = 7$ and $n_C = 3$. Generally, gas-phase reactions with the OH radical are pressure independent (Klein et al. 1984). So, k_{OH} can be assumed to be pressure independent and is taken to be 1.27×10^{-11} cm^3 molecule^{-1} s^{-1} at 760 Torr, while k_{OH*} is taken to be 7.72×10^{-12} cm^3 molecule^{-1} s^{-1}. Substituting the values (Table S1 of supplementary material) into Eq. (11), the estimated POCPs of DXL turns out to be 36 over northwestern European conditions and 38 for US urban conditions. Considering the POCP for ethene to be 100, POCP values for 1,3-dioxolane in both the conditions are lower. However, POCP values are well above the threshold (10) determined in the 2010 report of the world meteorological organization (Forster et al. 2010). Hence, we believe that 1,3-dioxolane will have a moderate contribution towards tropospheric ozone formation.

4 Conclusions

Oxidation by tropospheric oxidants, photodissociation, and wet deposition are known to be the major removal processes for any VOC from the troposphere. Photodissociation of 1,3-dioxolane in the tropospheric solar emission range is negligible as the compound does not absorb above 200 nm (Roquitte 1966). Being soluble in water, there is a good possibility of 1,3-dioxolane being washed out by precipitation. Its Henry law constant is reported to be 41.66 M atm^{-1} (Cabani et al. 1971). Using the expression for the wet deposition lifetime from Henry law constant (Chen et al. 2003), the lifetime is found to be 5.9 years with respect to wet deposition (calculation shown in section S1 of supplementary material), which is much larger in comparison to oxidation by tropospheric oxidants. Hence, tropospheric degradation by oxidants is the most probable sink of 1,3-dioxolane. Absolute value of k_{OH} with 1,3-dioxolane at 298 ± 2 K is found to be $(1.27 \pm 0.03) \times 10^{-11}$ cm^3 molecule^{-1} s^{-1} which is in excellent agreement with the relative value of $(1.13 \pm 0.12) \times 10^{-11}$ cm^3 molecule^{-1} s^{-1}. Value of k_{Cl} with 1,3-dioxolane at 298 ± 2 K is found be $(1.64 \pm 0.60) \times 10^{-10}$ cm^3 molecule^{-1} s^{-1}. From the lifetimes calculated considering the tropospheric concentration of the oxidants, the OH radical oxidation is the primary removal channel for 1,3-dioxolane under ambient conditions with the lifetime of about 22 h. However, near marine boundary layer, the Cl atom oxidation dominates and the overall lifetime reduces to about 8 h. Such a short lifetime with respect to reaction with OH and Cl suggests that the concentration of 1,3-dioxolane does not build up in the atmosphere. As a result, its atmospheric impact is locally concentrated on its emission zones. Formic acid, 1,2-ethanediol monoformate, and ethylene carbonate are observed as major products in Cl as well as OH oxidation, suggesting similar mechanism of reaction of 1,3-dioxolane for both the oxidants. 1,3-dioxolane may contribute as one of the sources of formic acid in the atmosphere. This is particularly important from the atmospheric point of view as formic acid leads to the formation of atmospheric aerosols (Aloisio et al. 2002). What's more, the POCP value of 1,3-dioxolane is calculated to be 36 and 38 over northwestern European conditions and US urban conditions, respectively. The POCP value being greater than the threshold (10) suggests the contribution of 1,3-dioxolane to tropospheric ozone formation.

The radiative efficiency and global warming potential (100-year horizon) of this compound is found to be 0.095 W m^{-2} ppb^{-1} and 0.18, respectively, suggesting negligible radiative burden on the atmosphere.

Supplementary Information The online version contains supplementary material available at https://doi.org/10.1007/s10874-023-09446-7.

Acknowledgements The authors are thankful to Dr. P.D. Naik for his keen interest and encouragement during the course of the work. The authors thank Bhabha Atomic Research Centre, Government of India for the financial support.

Author's contribution Anmol Virmani did the experimental work and wrote the original draft. Mohini P. Walavalkar and Asmita Sharma validated the results. Sumana Sengupta did the theoretical analysis. Ankur Saha and Awadhesh Kumar conceptualized and designed the methodology, reviewed and edited the manuscript.

Funding This work is funded by Bhabha Atomic Research Centre, India.

Data availability The data will be provided on request.

Code availability Not applicable.

Declarations

Ethics approval Not applicable.

Consent to participate Not applicable.

Consent for publication Not applicable.

Conflicts of interest The authors declare that they have no known competing financial interests or personal relationships that could have influenced the work reported in this paper.

References

Aloisio, S., Hintze, P.E., Vaida, V.: The hydration of formic acid. J. Phys. Chem. A **106**, 363–370 (2002). https://doi.org/10.1021/jp012190l

Andrei, G., Carter, K., Janeba, Z., Sampath, A., Schang, L.M., Tarbet, E.B., Hodge, R.A.V., Bray, M., Esté, J.A.: Highlights of the 30th International Conference on Antiviral Research. Antiviral Res. **145**, 184–196 (2017). https://doi.org/10.1016/j.antiviral.2017.07.017

Andrews, B.K.: 1, 3,-dioxolane, an alternative to formalin as a standard for formaldehyde. Textil. Res. J. **57**, 705–710 (1987). https://doi.org/10.1177/004051758705701205

Atkinson, R., Aschmann, S.M.: Kinetics of the gas phase reaction of Cl atoms with a series of organics at 296 ± 2 K and atmospheric pressure. Int. J. Chem. Kinet. **1**, 33–41 (1985). https://doi.org/10.1002/kin.550170105

Cabani, S., Conti, G., Lepori, L.: Thermodynamic study on aqueous dilute solutions of organic compounds. Part 2.—Cyclic ethers. Trans. Faraday Soc. **67**, 1943–1950 (1971). https://doi.org/10.1039/TF9716701943

Calve, S.L., Mellouki, A., Bras, G.L.: Kinetic studies of OH reactions with propylal, butylal and 1,3-dioxolane. Phys. Chem. Chem. Phys. **4**, 5622–5626 (2002). https://doi.org/10.1039/B206723D

Calvert, J.G., Atkinson, R., Becker, K.H., Seinfeld, J.H., Wallington, T.J., Yarwood, G.: The Mechanisms of Atmospheric Oxidation of the Aromatic Hydrocarbons. Oxford University Press, New York (2002)

Chen, L., Takenaka, N., Bandow, H., Maeda, Y.: Henry's law constants for C2–C3 fluorinated alcohols and their wet deposition in the atmosphere. Atmos. Environ. **37**, 4817–4822 (2003). https://doi.org/10.1016/j.atmosenv.2003.08.002

Chen, R., Jiang, Y., Li, J., An, Z., Chen, X., Chen, P.: Dielectric and optical anisotropy enhanced by 1,3-dioxolane terminal substitution on tolane-liquid crystals. J. Mater. Chem. C **3**, 8706–8711 (2015). https://doi.org/10.1039/C5TC01712B

Cheremisinoff, N.P.: Industrial Solvents Handbook, Revised And Expanded (2nd ed.). CRC Press, Marcel Dekker, New York (2003). https://doi.org/10.1201/9780203911334

Daranlot, J., Bergeat, A., Caralp, F., Caubet, P., Costes, M., Forst, W., Loison, J.C., Hickson, K.M.: Gas-phase kinetics of hydroxyl radical reactions with alkenes: experiment and theory. ChemPhysChem **11**, 4002–4010 (2010). https://doi.org/10.1002/cphc.201000467

Derwent, R.G., Jenkin, M.E.: Hydrocarbons and the long-range transport of ozone and pan across Europe. Atmos. Environ. A, Gen. Top. **25**, 1661–1678 (1991). https://doi.org/10.1016/0960-1686(91)90025-3

Dinis, C.M.F., Geiger, H., Wiesen, P.: Kinetics of the reactions of OH(X2Π) radicals with 1,3-dioxolane and selected dialkoxy methanes. Phys. Chem. Chem. Phys. **3**, 2831–2835 (2001). https://doi.org/10.1039/B100181G

Dolislager, L.J.: The effect of California's wintertime oxygenated fuels program on ambient carbon monooxide concentrations. J. Air Waste Manage. **47**, 775–783 (1997). https://doi.org/10.1080/10473289.1997.10463935

Forster, P.M., Thompson, D.W.J., Baldwin, M., Chipperfifield, M.P.: Stratospheric Changes and Climate,Chapter 4 in Scientifific Assessment of Ozone Depletion: 2010, Global Ozone Research and Monitoring Project—Report No. 52. Cambridge University Press, Geneva, Switzerland (2010)

Frisch, M.J., Trucks, G.W., Schlegel, H.B., Scuseria, G.E.: Gaussian, Inc., Wallingford CT (2004)

Graedel, T.E., Hawkins, D.T., Claxton, L.D.: Atmospheric Chemical Compounds: Sources, Occurrence, and Bioassay. Academic Press, Orlando, Florida (1986)

Gupta, B.S., Fang, M.-Y., Lee, M.-J.: Separation of 1,3-dioxolane from its azeotropic aqueous solution by using Good's buffer ionic liquid [TMA][EPPS]. Fluid Phase Equil. **418**, 119–124 (2016). https://doi.org/10.1016/j.fluid.2015.10.033

Hammond, G.S.: A Correlation of Reaction Rates. J. Am. Chem. Soc. **77**, 334–338 (1955). https://doi.org/10.1021/ja01607a027

Hasegawa, A.: Measurement of Ethylene Oxide in the Atmosphere. J. Environ. Chem. **11**, 11–15 (2001)

Hodnebrog, O., Etminan, M., Fuglestvedt, J.S., Marston, G., Myhre, G., Nielsen, C.J., Shine, K.P., Wallington, T.J.: Global warming potentials and radiative efficiencies of halocarbons and related compounds: a comprehensive review. Rev. Geophys. **51**, 301–378 (2013). https://doi.org/10.1002/rog.20013

Illés, A., Rózsa, Z.B., Thangaraj, R., Gombos, E.D., Dóbé, S., Giri, B.R., Szőri, M.: An experimental and theoretical kinetic study of the reactions of hydroxyl radicals with tetrahydrofuran and two deuterated tetrahydrofurans. Chem. Phys. Lett. **776**, 138698 (2021)

Jenkin, M.E., Derwent, R.G., Wallington, T.J.: Photochemical ozone creation potentials for volatile organic compounds: rationalization and estimation. Atmos. Environ. **163**, 128–137 (2017). https://doi.org/10.1016/j.atmosenv.2017.05.024

Kawade, M., Sharma, A., Srinivas, D., Saha, A., Upadhyaya, H.P., Kumar, A., Naik, P.D:. Rate coefficients of hydroxyl radical reaction with dimethyl ether over a temperature range of 257–333 K. Chem. Phys. Lett. **706**, 558–563 (2018a), https://doi.org/10.1016/j.cplett.2018.06.065

Kawade, M.N., Srinivas, D., Upadhyaya, H.P.: Gas phase OH radical reaction with 2-Chloroethyl Vinyl Ether in the 256–333 K temperature range: A combined LP-LIF and computational Study. ChemistrySelect **23**, 5910–5919 (2018b). https://doi.org/10.1002/slct.201800885

Kawade, M.N., Srinivas, D., Upadhyaya, H.P.: Kinetics of Gas Phase OH Radical Reaction with Thiophene in the 272–353 K Temperature Range: A Laser Induced Fluorescence Study. Chem. Phys. Lett. **682**, 154–159 (2017). https://doi.org/10.1016/j.cplett.2017.05.07

Klein, T., Barnes, I., Becker, K.H., Fink, E.H., Zabel, F.: Pressure dependence of the rate constants for the reactions of C_2H_4 and C_3H_8 with OH radicals at 295 K. J. Phys. Chem. **88**, 5020–5025 (1984)

Küçük, H.B., Yusufoğlu, A., Mataracı, E., Döşler, S.: Synthesis and biological activity of new 1,3-Dioxolanes as potential antibacterial and antifungal compounds. Molecules **16**, 6805–6815 (2011). https://doi.org/10.3390/molecules16086806

Lohmann, R., Breivik, K., Dachs, J., Muir, D.: Global fate of POPs: Current and future research directions. Environ. Pollut. **150**, 150–165 (2007)

McGillen, M.R., Carter, W.P.L., Mellouki, A., Orlando, J.J., Picquet-Varrault, B., Wallington, T.J.: Database for the kinetics of the gas-phase atmospheric reactions of organic compounds. Earth Syst. Sci. Data **12**, 1203–1216 (2020). https://doi.org/10.5194/essd-12-1203-2020

Moriarty, J., Sidebottom, H., Wenger, J., Mellouki, A., Bras, G.L.: Kinetic studies on the reactions of hydroxyl radicals with cyclic ethers and aliphatic diethers. J. Phys. Chem. A **107**, 1499–1505 (2003)

Moriarty, J., Wenger, J., Sidebottom, H.: Kinetic studies on the reactions of hydroxyl radicals with cyclic ethers. WIT Trans. Ecol. Environ. **28**, 115–119 (1999). https://doi.org/10.2495/EURO990221

Ovsyannikova, M.N., Vol'eva, V.B., Belostotskaya, I.S., Komissarova, N.L., Malkova, A.V., Kurkovskaya, L.N.: Antibacterial activity of substituted 1,3-Dioxolanes. Pharm. Chem. J. **47**, 142–145 (2013). https://doi.org/10.1007/s11094-013-0913-6

Pandit, S., B. Hornung, Dunning, G.T., Preston, T.J., Brazener, K., Orr-Ewing, A.J.: Primary vs secondary H- atom abstraction in the Cl-Atom reaction with n-Pentane. Phys. Chem. Chem. Phys. **19**, 1614–1626 (2017). https://doi.org/10.1039/C6CP07164C

Persis S. de, Dollet A., Teyssandier F.: Pressure Dependence of Gas-Phase Reaction Rates. J. Chem. Educ., **81**, 6, 832 (2004). https://doi.org/10.1021/ed081p832

Porter, E., Wenger, J., Treacy, J., Sidebottom, H., Mellouki, A., Téton, S., LeBras, G.: Kinetic studies on the reactions of hydroxyl radicals with diethers and hydroxyethers. J. Phys. Chem. A **101**, 5770–5775 (1997). https://doi.org/10.1021/jp971254i

Prinn, R.G., Huang, J., Weiss, R.F., Cunnold, D.M., Fraser, P.J.: Evidence for substantial variations of atmospheric hydroxyl radicals in the past two decades. Science **292**, 1882–1888 (2001). https://doi.org/10.1126/science.1058673

Roquitte, B.C.: The photochemistry of 1,3-Dioxolane. J. Phys. Chem. **70**, 2863–2868 (1966). https://doi.org/10.1021/j100881a023

Sauer, C.G., Barnes, I., Becker, K.H., Geiger, H., Wallington, T.J., Christensen, L.K., Platz, J., Nielsen, O.J.: Atmospheric chemistry of 1,3-Dioxolane: Kinetic, mechanistic, and modeling Study of OH radical initiated oxidation. J. Phys. Chem. A **103**, 5959–5966 (1999). https://doi.org/10.1021/jp991025r

SenGupta, S., Indulkar, Y., Kumar, A., Dhanya, S., Naik, P.D.: Kinetic study of the gas-phase reaction of hydroxyl radical with $CF_3CH_2OCH_2CF_3$ using the laser photolysis-laser induced fluorescence method. Int. J. Chem. Kinet. **42**, 519–525 (2010). https://doi.org/10.1002/kin.20507

Schure, A.F.H. T., Larsson, P., Agrell, C., Boon, J.P.: Atmospheric transport of polybrominated diphenyl ethers and polychlorinated biphenyls to the Baltic Sea. Environ. Sci. Technol. **38**, 1282–1287 (2004). https://doi.org/10.1021/es0348086

Senosiain, J.P., Klippenstein, S.J., Miller, J.A.: Reaction of ethylene with hydroxyl radicals: A theoretical study. J. Phys. Chem. A **110**, 6960–6970 (2006). https://doi.org/10.1021/jp0566820

Sharma, A., Pushpa, K.K., Dhanya, S., Naik, P.D., Bajaj, P.N.: Rate constants for the gas-phase reactions of chlorine atoms with 1,4-cyclohexadiene and1,5- cyclooctadiene at 298 K. Int. J. Chem. Kinet. **43**, 431–440 (2011). https://doi.org/10.1002/kin.20567

Song, J., Zello, V., Boehman, A.L., Waller, F.J.: Comparison of the Impact of Intake Oxygen Enrichment and Fuel Oxygenation on Diesel Combustion and Emissions. Energ. Fuel **18**, 1282–1290 (2004)

Spicer, C.W., Chapman, E.G., Finlayson-Pitts, B.J., Plastridge, R.A., Hubbe, J.M., Fast, J.D., Berkowitz, C.M.: Unexpectedly high concentrations of molecular chlorine in coastal air. Nature **394**, 353–356 (1998). https://doi.org/10.1038/28584

Squillace, P.J., Zogorski, J.S., Wilber, W.G., Price, C.V.: Preliminary assessment of the occurrence and possible sources of MTBE in groundwater in the United States, 1993±1994. Environ. Sci. Technol. **30**, 1721–1730 (1996). https://doi.org/10.1021/es9507170

Su, Y., Hung, H., Sverko, E., Fellin, P., Li, H.: Multi-year measurements of polybrominated diphenyl ethers (PBDEs) in the Arctic atmosphere. Atmos. Environ. **41**, 8725–8735 (2007). https://doi.org/10.1016/j.atmosenv.2007.07.032

Szori, M., Abou-Abdo, T., Fittschen, C., Csizmadia, I.G., Viskolcz, B.: Allylic hydrogen abstraction: H-abstraction from 1,4 type polyalkenes as a model for free radical trapping by polyunsaturated fatty acids (PUFAs). Phys. Chem. Chem. Phys. **9**, 1931–1940 (2007). https://doi.org/10.1039/B613048H

Torré, J.-P., Haillot, D., Rigal, S., Lima, R.D.S., Dicharry, C., Bedecarrats, J.P.: 1, 3 Dioxolane versus tetrahydrofuran as promoters for CO_2- hydrate formation: Thermodynamics properties, and kinetics in presence of sodium dodecyl sulfate. Chem. Eng. Sci. **126**, 688–697 (2015). https://doi.org/10.1016/j.ces.2015.01.018

Wallington, T.J., Hurley, M.D., Ball, J.C., Straccia, A.M., Platz, J., Christensen, L.K., Sehested, J., Nielsen, O.J.: Atmospheric chemistry of dimethoxymethane ($CH_3OCH_2OCH_3$): Kinetics and mechanism of its reaction with OH radicals and fate of the alkoxy radicals $CH_3OCHO(\bullet)OCH_3$ and $CH_3OCH_2OCH_2O(\bullet)$. J. Phys. Chem. A **101**, 5302–5308 (1997). https://doi.org/10.1021/jp9631184

Wang, Y., Xu, R., Xiao, B., Lv, D., Peng, Y., Zheng, Y., Shen, Y., Chai, J., Lei, X., Luo, S., Wang, X., Liang, X., Feng, J., Liu, Z.: A poly(1,3-dioxolane) based deep-eutectic polymer electrolyte for high performance ambient polymer lithium battery. Mater. Today Phys. **22**, 100620 (2022). https://doi.org/10.1016/j.mtphys.2022.100620

Zhang, R.M., Truhlar, D.G., Xu, X.: Kinetics of the toluene reaction with OH Radical. Research **19**, 5373785 (2019). https://doi.org/10.34133/2019/5373785